J Solid State Electrochem (2012) 16:689–695
DOI 10.1007/s10008-011-1419-3

ORIGINAL PAPER

Electrochemical sensor using glassy carbon electrode modified with acylpyrazolone-multiwalled carbon nanotube composite film for determination of xanthine

Yun Song · Jinzhou Li

Received: 9 November 2010 / Revised: 20 April 2011 / Accepted: 25 April 2011 / Published online: 6 May 2011

Abstract In this work, an electrochemical sensor 1-phenyl-3-methyl-4-(2-furoyl)-5-pyrazolone/multiwalled carbon nanotubes/glassy carbon electrode (GCE) was prepared for the determination of xanthine (XN) in the presence of an excess of uric acid. Cyclic voltammetry and differential pulse voltammetry were used to characterize the electrode. The oxidation of XN occurred in a well-defined peak having E_p 0.73 V in phosphate buffer solution of pH 6.0. Compared with the bare GCE, the electrochemical sensor greatly enhanced the oxidation signal of XN with negative shift in peak potential about 110 mV. Based on this, a sensitive, rapid, and convenient electrochemical method for the determination of XN has been proposed. Under the optimized conditions, the oxidation peak current of XN was found to be proportional to its concentration in the range of 0.3~50 μM with a detection limit of 0.08 μM. The analytical utility of the proposed method was demonstrated by the direct assay of XN in urine samples and was found to be promising at our preliminary experiments.

Keywords Acylpyrazolone · Multiwalled carbon nanotube · Composite film · Xanthine · Uric acid

Introduction

Xanthine (XN) is an intermediate of the purine metabolism and is produced after adenosine triphosphate decomposition [1]. The physiological conversion of XN by xanthine oxidase is of considerable importance in biochemical and clinical diagnosis [1, 2]. Extreme abnormal levels of XN in body fluids are symptoms of several diseases, such as renal failure [1]. Uric acid (UA) is the primary end product of purine metabolism. It has been found to be associated with many diseases such as hyperuricemia, gout, leukemia, and pneumonia [3].

Several enzymatic methods for the determination of XN have been reported [4–6]. However, electrochemical sensor has obtained wide application in biomedical monitoring. For example, a nanostructured polymer film modified glassy carbon electrode (GCE) [1], an ultrathin polymer film of 5-amino-1,3,4-thiadiazole-2-thiol modified GCE [2], a mesoporous SiO_2 sensor [7], and a preanodized nontronite-coated, screen-printed electrode [8] have been published for the detection of XN. It is well known that UA coexists with XN in our body fluids and its concentration is much higher than that of XN. Therefore, it is very important to develop simple and rapid methods for XN selective determination in routine analysis.

Since the discovery of carbon nanotubes (CNTs) in 1991 [9], they have been the target of numerous investigations, owing to their good electrical conductivity, high chemical stability, and extremely high mechanical strength [10, 11]. The CNT mechanism of charge transport can vary from semiconducting type to metallic type, depending on their radius and helical structure [12]. In addition, the subtle electronic behavior reveals that CNTs have the ability to promote electron-transfer reaction with electroactive species in solution. They have been studied extensively for a large variety of applications, particularly for solid-state chemical and biological sensors [13, 14]. All these fascinating properties make CNTs as a suitable candidate for the modification of electrodes [15, 16].

Y. Song · J. Li (✉)
College of Chemistry and Chemical Engineering,
Harbin Normal University,
Harbin 150025, People's Republic of China
e-mail: lijinzhou20@163.com

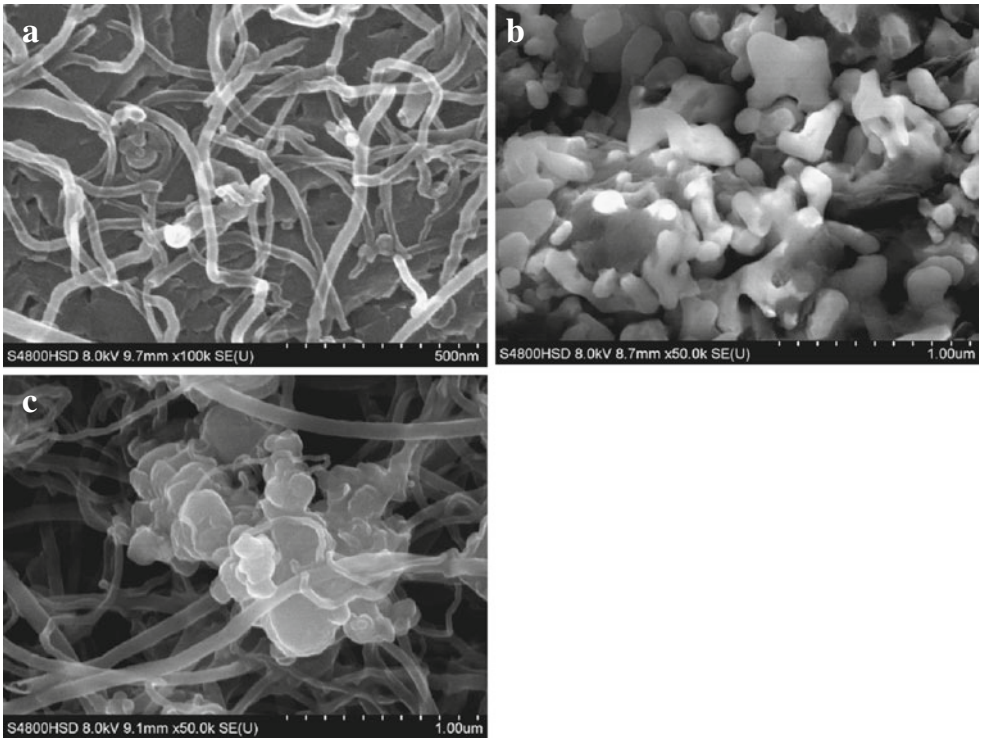

Fig. 1 SEM images of the surface of **a** MWNTs/GCE, **b** HPMαFP/GCE, **c** HPMαFP/MWNTs/GCE

1-Phenyl-3-methyl-4-(2-furoyl)-5-pyrazolone (HPMαFP) is a kind of β-diketo compound. The neutral acylpyrazolones may exist with several possible tautomeric forms as reported [17, 18]. The enol form OH is weakly acidic, as a surfactant, which makes it suitable for electrochemical analysis [19, 20]. Due to the aromaticity of HPMαFP, they can adsorb onto the surfaces of the CNTs through π–π force to form the composite film [21]. To the best of our knowledge, there are no reports on the fabrication of the HPMαFP/multiwalled carbon nanotubes (MWNTs)/GCE and its response on XN in the presence of UA.

In this paper, MWNTs are adopted to couple with the HPMαFP to form the composite electrode. Combination of the advantages of these two materials can accelerate the electron-transfer rate, improve the electrochemical character, and enhance the active surface area of the electrode. This work aims to investigate the electrochemical behavior of XN on the composite electrode and its possible applicability for XN determination in urine samples.

Experimental

Reagents

The multiwalled carbon nanotubes came from Shenzhen Nanotech Port Co. Ltd. (Shenzhen, China). HPMαFP was synthesized according to the method proposed by Dong [22] with further purification, and a standard solution (0.01 M) of HPMαFP was prepared by anhydrous ethanol solution. XN and UA were purchased from Sigma and were used as received. Phosphate buffer solution (PBS) was prepared using 0.1 M Na_2HPO_4 and NaH_2PO_4. All other chemicals used in this investigation were of analytical grade, and the solutions were prepared by doubly distilled water.

Apparatus

The morphological features of electrode surfaces were observed by a scanning electron microscopy (SEM,

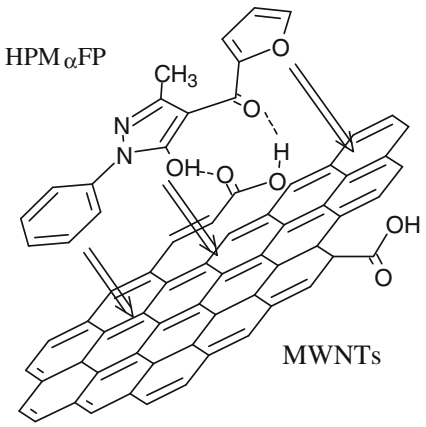

Scheme 1 The interaction between MWNTs and HPMαFP

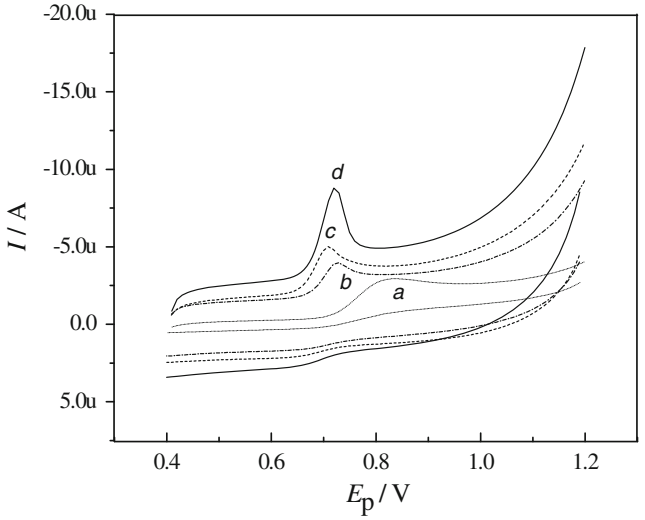

Fig. 2 Cyclic voltammograms of 1.0×10^{-5} M XN (pH=6.0) at **a** bare GCE, **b** HPMαFP/GCE, **c** MWNTs/GCE, **d** HPMαFP/MWNTs/GCE. Scan rate, 100 mV s^{-1}

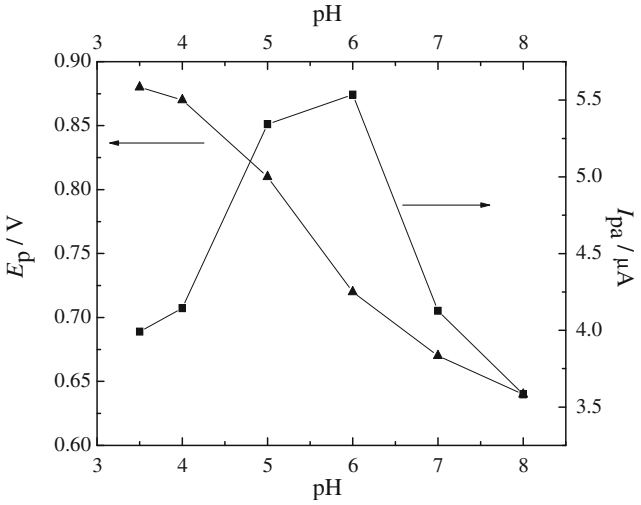

Fig. 3 Influence of pH on the peak current (I_{pa}) and peak potential (E_p) of XN

HITACHI S-4800). All electrochemical measurements were performed on a CHI-650A electrochemical workstation (Shanghai CH Instruments, China). A conventional three-electrode system equipped with a saturated calomel electrode (SCE) as the reference electrode, a platinum wire electrode served as the auxiliary electrode and a GCE, a MWNTs/GCE, or a MWNTs/HPMαFP/GCE served as the working electrodes. All potentials were referred to the SCE.

Preparation of MWNTs modified GCE

MWNTs crude material was agitated in an ultrasonic bath with 3 M nitric acid for 2 h and refluxed in 5 M HCl for 6 h at 40 °C, and finally, thoroughly washed with water to obtain a neutral state and dried in oven at 120 °C. Such MWNTs have functional surfaces, such as –OH and –COOH groups. The MWNTs–*N*,*N*-dimethylformamide (DMF) suspension was achieved by adding 5 mg MWNTs in 5 mL DMF and sonicating for 30 min. The GCE was polished with 1.0 and 0.3 micron alumina slurry on chamois leather, rinsed thoroughly with nitric acid (1:1), anhydrous ethanol, and doubly distilled water, respectively. Then, it was dried and ready for use. The cast film was prepared by placing 5 μL MWNTs/DMF suspensions on GCE and dried under an infrared lamp.

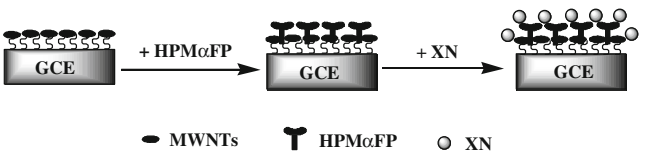

Scheme 2 The interaction between XN and HPMαFP/MWNTs/GCE

Preparation of MWNTs/HPMαFP/GCE

The dried MWNTs/GCE was carefully coated with appropriate amount of HPMαFP solution and left for the solvent to evaporate at room temperature in the air.

Experimental procedure

PBS 0.1 M (pH 6.0) with certain amount of XN was transferred into a cell, and the three-electrode system was installed in it. High-purity N_2 was used to remove oxygen. Cyclic voltammograms were recorded between 0.4 and 1.2 V at scan rate of 100 mV s^{-1}. All experiments were carried out at room temperature (298±2 K).

Results and discussion

SEM studies of the modified electrodes

The morphology of the modified electrodes was examined by SEM. Figure 1 displays typical images of MWNTs, HPMαFP, and HPMαFP/MWNTs films assembled onto GCE. As it can be observed, the MWNTs and HPMαFP dispersed over the glassy carbon surface, and at the HPMαFP/MWNTs film, HPMαFP adsorbed on the surface of MWNTs. The reasons were concluded in the

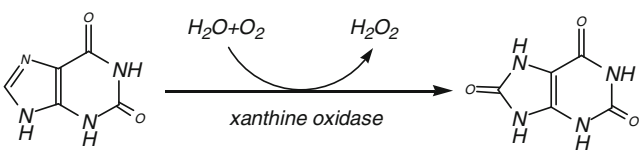

Scheme 3 The reaction mechanism for XN

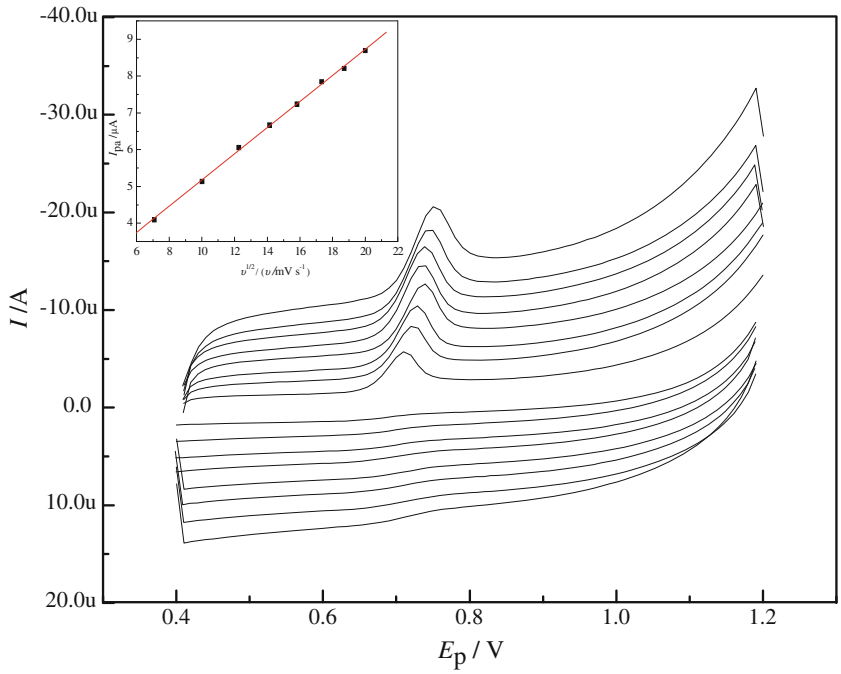

Fig. 4 Cyclic voltammograms of 1.0×10^{-5} M XN in 0.10 M PBS (pH 6.0) at various scan rates (from inner to outer), 50 to 400 mV s^{-1}. *Inset* plot of the I_{pa} vs. υ

following aspects. The π–π interaction between the aromaticity of HPMαFP and hexagonal carbon structure of MWNTs was attributed to the easy arrival of HPMαFP to the surface of MWNTs [21]. Moreover, at the end of MWNTs, some active functional groups maybe existed, such as carbonyl. So, the intermolecular effect (hydrogen bond) was formed between MWNTs and HPMαFP (as shown in Scheme 1).

Effect of HPMαFP and MWNT amount

Effect of different HPMαFP and MWNT amount on peak current of XN was investigated. Experiments showed that the electrode surface area increased noticeably with the augment of quantity of MWNT. However, too much MWNT may be more easily abraded from the surface of GCE. So, 5 μL MWNT was selected. On the other hand,

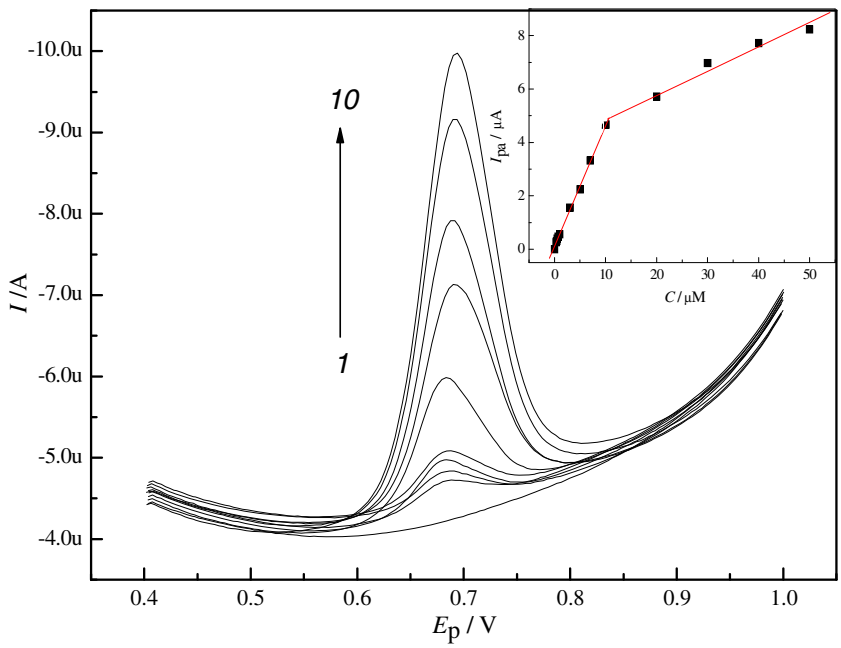

Fig. 5 Differential pulse voltammograms of HPMαFP/MWNTs/GCE in 0.10 M PBS (pH 6.0) containing different concentration of XN in the range of 0–50 μM. *Inset* plot of the peak current vs. the concentration of XN. Pulse width=0.05 s, amplitude=0.05 V, sample period=0.0167 s, and pulse period=0.2 s

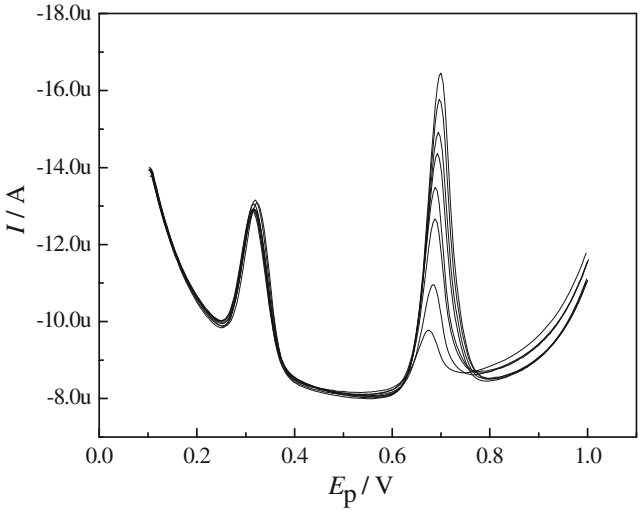

Fig. 6 DPVs obtained for the increment of 5 μM XN to 20 μM UA in 0.1 M PBS at HPMαFP/MWNTs/GC electrode. DPV parameters are the same as in Fig. 5

the oxidation peak current gradually increased with the augment of quantity of HPMαFP. When the HPMαFP was beyond 0.6 μL, the peak current decreased. This was due to the surface of MWNTs/GCE casted too thick to hamper the charge exchange. To sum up, 5 μL MWNT and 0.6 μL HPMαFP was selected in the following experiments and the maximum electrocatalytic response on XN was achieved. Here the data have not been showed.

Voltammetric behavior of XN at HPMαFP/MWNTs/GCE

The electrochemical behavior of XN was studied. Figure 2 depicted the CVs of 1.0×10^{-5} M XN in pH 6.0 PBS at four different working electrodes. At the bare GCE (Fig. 2a), it can be seen that an irreversible oxidation peak appeared at 0.84 V. At the HPMαFP/GCE (Fig. 2b), the oxidation peak located at 0.73 V. The oxidation peak potential (E_{pa}) was negatively shifted for 0.11 V, and the oxidation peak current (I_{pa}) increased clearly. Although both the oxidation peak current and potential of XN increased and moved negatively slightly at MWNTs (Fig. 2c) modified electrode, the peak current was still smaller than that at HPMαFP/MWNTs/GCE (Fig. 2d). From the comparison of voltammograms of XN, it can be observed that the peak current at HPMαFP/MWNTs/GCE was more than two times higher than the sum of response currents at HPMαFP/GCE or MWNTs/GCE. The above results indicated that the composite film sensor exhibited the synergistic effect including high conductivity, fast electron-transfer rate, and inherent catalytic ability. This phenomenon was probably due to the hydrogen bond between XN and HPMαFP or XN and MWNTs, which can remarkably increase the accumulation amount of XN (as shown in Scheme 2).

Effect of pH

Influence of pH on electrochemical behavior of 1.0×10^{-5} M XN at HPMαFP/MWNTs/GCE was investigated in the pH range from 3.5 up to 8.0. The results were shown in Fig. 3. The variation of E_{pa} with pH can provide valuable information on the XN oxidation process. The peak potential was found to shift negatively as pH was increased. The slope of the E_{pa} vs. pH plot being 58 mV per pH unit. According to the equation: $-59\chi/n=-58$, where χ is the hydrogen ion participating the electrode reaction and n is the electron-transfer number. So, the loss of electrons was accompanied by the loss of an equal amount of protons and $\chi=n=2$ [23]. The reaction mechanism for XN was shown in Scheme 3[8, 24].

The effect of buffer solution pH on the oxidation peak current was also studied. The pH values around 6.0 should provide the highest oxidation currents justifying the selection of pH 6.0 for the subsequent experiments using the HPMαFP/MWNTs/GCE film electrode.

Effect of sweep rate

The effect of scan rate on the voltammetric response for the oxidation of 1.0×10^{-5} M XN on the HPMαFP/MWNTs/GCE was investigated from 50 to 400 mV s^{-1} (shown in Fig. 4). The cyclic voltammetric results indicated that the anodic peak current varied linearly with the square root of the scan rate according to the equation: $I_{pa}(\text{in microampere})=-1.616-0.3558\upsilon^{1/2}$, with a linear correlation coefficient of 0.9994 (n=8). Such behaviors revealed that the oxidation of XN on the surface of HPMαFP/MWNTs/GCE was diffusion controlled.

Analytical curve for XN

Linear range and limit of detection

Differential pulse voltammetry (DPV) technique was employed to develop a voltammetric method for determi-

Table 1 The tolerance limit of interfering substances on CV determination of XN (1×10^{-5} M) using HPMαFP/MWNTs/GCE

Substance	Tolerance limit ($\times10^{-5}$ M)
K^+, Na^+, Cl^-, $H_2PO_4^-$, HPO_4^{2-}, PO_4^{3-}, SO_4^{2-}, Ac^-	200
Cytosine, L-leucine, DL-serine, guanine, DL-phenylalanine	100
Adenine, thymine	50

Table 2 Results of analysis of XN in human urine samples

Samples	Original (μM)	Added (μM)	Found (μM)	Recoveries (%)
Urine 1	1.01	1	1.98	98.51
		3	4.10	102.24
Urine 2	1.24	1	2.24	100.00
		3	4.15	97.88

nation of XN because of its higher sensitivity and excellent resolution. Voltammograms at these concentrations were shown in Fig. 5, and two linear calibration graphs were obtained (inset, Fig. 5). The initial linear portion increased from 0.3~10 μM with a linear regression equation of I_{pa} (in microampere)=0.454C (in micromolar)+0.11 (r=0.9989). The second linear segment is from 10 up to 50 μM with a linear regression equation of I_{pa} (in microampere)=0.091C (in micromolar)+3.917 (r=0.9874). The detection limit (S/N=3) was found to be 0.08 μM. This detection limit was lower, and the sensitivities were higher than those obtained by other electrochemical methods [1, 7, 25]

Determination of XN in the presence of UA

The main objective of the present study is to selectively determine XN in the presence of UA. Figure 6a showed the DPVs for the increment of 5 μM XN in the presence of 20 μM UA in 0.1 M PBS (pH=6.0). During the anodic sweep from 0.1 to 1.0 V, two oxidation peaks at 0.32 and 0.68 V were observed at the HPMαFP/MWNTs/GCE. The oxidation current of XN was linearly increases by its concentration from 1 to 40 μM with a correlation coefficient of 0.9961. These results indicated that HPMαFP/MWNTs modified electrode was highly selective towards the oxidation of XN and detection of very low concentration XN was possible in the presence of an excess of UA, and it was also possible in the presence of 200-fold excess of ascorbic acid (AA). However, by this modified electrode, AA and UA have the similar oxidation potentials, where the cyclic voltammograms were omitted.

Interferences

Prior to the application of proposed method on real samples, it was vital to investigate the effect of the interfering ions or biomolecules on the recovery percentage of XN. The tolerance limit was defined as the maximum concentration of the interfering substance that caused an error less than ±5% for determination of XN. Under the optimum experimental conditions, the effects of potential interferents on the voltammetric response of 1×10^{-5} M XN as a standard were evaluated. The tolerable limits of interfering substance were given in Table 1. Generally, the results point out a high selectivity for XN over many common inorganic ions and biomolecules.

Detection of XN in urine samples

The practical application of HPMαFP/MWNTs/GCE was tested by measuring the concentration of XN in human urine samples. A quantitative analysis can be carried out by adding the standard solution of XN into the detect system. The human urine samples were collected from laboratory co-workers and were diluted to 50 times with pH 6.0 PBS without any treatment. The DPV of XN showed oxidation peak at 0.67 V. To confirm the observed oxidation peak of XN, the urine sample was spiked with known concentration of commercial XN. The increasing peak current at 0.67 V after the addition of XN made certain that the observed oxidation peak was due to the oxidation of XN. The detection results of two urine samples obtained were listed in Table 2. The recovery determined in the range from 97.88% to 102.24% indicated that this method could be efficiently used for the determination of XN in real samples.

Conclusions

HPMαFP/MWNTs/GCE were prepared and had been used to investigate the electrochemical behaviors of XN. It was a diffusion-controlled irreversible process with two electrons and two protons. This modified electrode exhibited high electrocatalytic activities towards the oxidation of XN by significantly decreasing their oxidation overpotentials and enhancing the peak currents. The HPMαFP/MWNTs/GCE was also used for the determination of XN in the presence of high concentration of UA by DPV. This electrochemical sensor showed excellent selectivity and high sensitivity. A well separation of oxidation peaks of XN and UA can be achieved. Also, the proposed method could be applied to the determination of XN in urine samples with satisfactory results.

Acknowledgment This work was supported by grants from the Nature Science Foundation of Heilongjiang Province, People's Republic of China (No. B201004) and the Scientific and Technical Development Foundation of Harbin Normal University (No. 08XYG-12).

References

1. Palraj K, Abraham SJ (2010) Talanta 80:1686–1691
2. Palraj K, Abraham SJ (2009) Anal Chim Acta 647:97–103
3. Guilbault GG (1984) Analytical uses of immobilized enzymes. Marcel Dekker, New York
4. Villalonga R, Matos M, Cao R (2007) Electrochem Commun 9:454–458
5. Kirgoz UA, Timur S, Wang J, Telefoncu A (2004) Electrochem Commun 6:913–916
6. Arslan F, Yaşar A, Kılıç E (2006) Artif Cell Blood Substit Biotechnol 34:113–128
7. Sun D, Zhang Y, Wang FR, Wu KB, Chen JW, Zhou YK (2009) Sensor Actuator B Chem 141:641–645
8. Zen JM, Lai YY, Yang HH, Senthil KA (2002) Sensor Actuator B Chem 84:237–244
9. Iijima S (1991) Nature 354:56–58
10. Wildgoose GG, Banks CE, Leventis HC, Compton RG (2006) Microchim Acta 152:187–214
11. Iijima S (2002) Phys B 323:1–5
12. Yang LJ, Tang C, Xiong HY, Zhang XH, Wang SF (2009) Bioelectrochemistry 75:158–162
13. Moraes FC, Mascaro LH, Machado SAS, Brett CMA (2009) Talanta 79:1406–1411
14. Wu YH (2010) Food Chem 121:580–584
15. Andrews R, Weisenberger MC (2004) Curr Opin Solid State Mater Sci 8:31–37
16. Manisankar P, Abirama Sundari PL, Sasikumar R, Palaniappan SP (2008) Talanta 76:1022–1028
17. Nishihama S, Hirai T, Komasawa I (2001) Ind Eng Chem Res 40:3085–3091
18. Marchetti F, Pettinari C, Pettinari R (2005) Coord Chem Rev 249:2909–2945
19. Ghoneim MM, El-Desoky HS, Amer SA, Rizk HF, Habazy AD (2008) Dyes Pigments 77:493–501
20. Zhang D, Li JZ (2008) Anal Lett 41:2832–2843
21. Li FH, Chai J, Yang HF, Han DX, Niu L (2010) Talanta 81:1063–1068
22. Dong XC, Liu FC, Zhao YL (1983) Acta Chim Sinica 41:848–852
23. Wei S, Li YZ, Duan YY, Jiao K (2008) Biosens Bioelectron 24:988–993
24. Anik U, Cubukcu M (2008) Turk J Chem 32:711–719
25. Kumar AS, Swetha P (2010) J Electroanal Chem 642:135–142